The Demagnetization Harmonics Generation Mechanism in Permanent Magnet Machines with Concentrated Windings

The Demagnetization Harmonics Generation Mechanism in Permanent Magnet Machines with Concentrated Windings

Konstantinos N. Gyftakis, *Senior Member, IEEE*, Syidy Ab Rasid, *Student Member, IEEE,* Giorgos A. Skarmoutsos, *Student Member, IEEE,* and Markus Mueller

***Abstract*—Partial demagnetization is a condition that may occur in Permanent Magnet machines due to overloading or thermal stress. When this happens, the magnetic field locally weakens leading to an asymmetry of the air-gap field. This asymmetry will cause harmonics, which will be expressed as extra losses and mechanical oscillations. Moreover, since the field becomes weaker, more current is required to serve the load leading to less efficiency, increased losses and consequently increase of the temperature, which will cause further progression of the demagnetization severity until a total machine breakdown. Several methods have been proposed in the literature for the online detection of the demagnetization, however they have not related the fault to the manufacturing characteristics of the machine, which play an important role on the expected harmonic index and the associated fault signatures. This paper presents for the first time a detailed analytical investigation of the expected harmonics in the stator current spectrum in case of demagnetization, as a function of the stator winding and number of poles. The analytical results are verified by extensive simulations via the finite element method and experimental testing.**

***Index Terms*—Condition monitoring, Demagnetization, Fault diagnosis, Permanent Magnet machines**

NOMENCLATURE

b, c, d, l, r, q, $\delta, \zeta, \lambda, \lambda'$: integer numbers
a_k: the sum between a and β
β_k: equal to 0.5 $\gamma(D)$
B: magnetic flux density
B_{AG}: magnetic flux density in the air-gap
D: demagnetization severity
$\mathcal{F}_m$: the Magneto-Motive Force (MMF)
F_{PM}: the MMF amplitude
f_{3ph_null}: voltage summation of phases under demagnetization
f_{dmg}: frequency locations of demagnetization harmonics
f_s: synchronous frequency
g: air-gap length
h_{PM}: permanent-magnet height
k: pulse wave series index
N: turn number of an armature coil
n: harmonic order
p: pole pair number
p': electrical angle factor or the number of coils
t: time
t_w: winding thickness
V_{dmg}: voltage in the stator coils due to the demagnetization
V_n, V_{nl}, V_{kl}: voltage amplitudes
V_{nk}: voltage of nth harmonic in the kth term
V_{2c_dmg}: voltage summation between two coils
V_{3c_dmg}: voltage demagnetization signatures due to three phases and multiple phase coils
$V_{3ph\_dmg\_1c}$: voltage demagnetization signatures due to three phases and 1 coil/phase
V_{3ph_dmg}: voltage summation of phases under demagnetization
α: constant related to the design parameters
β: constant related to the design parameters and demagnetization
γ: constant related to design parameters and demagnetization
$\mathcal{E}$: the Electromotive Force (EMF)
θ: space angle
Λ: air-gap permeance
Λ_{dmg}: relative permeance function under demagnetization
μ_o: permeability of free space
Φ: the magnetic flux
φ_n: the phase angle of the nth harmonic component
ω_r: the rotor radial frequency
ω_s: the synchronous radial frequency

I. INTRODUCTION

PERMANENT-MAGNET machines have many advantages over the conventional brushed synchronous machines, such as higher efficiency, torque density, better dynamic performance, simplest design structure, and lower maintenance demands [1], [2]. However, due to high instant armature reaction fields, operational temperatures, oxidation, and corrosion of materials, the operational point on the magnetic characteristic shifts under the knee point [3] causing demagnetization. Moreover, demagnetized motors demand higher stator current in order to produce the same torque, which leads to faster degradation of the stator insulation [4], [5]. Furthermore, partial demagnetization increases the higher force

All authors are with the School of Engineering and the Institute for Energy Systems, The University of Edinburgh, Edinburgh, EH9 3FB, UK (e-mail: k.n.gyftakis@ieee.org).

harmonic magnitude of components, leading to vibration and acoustic noise radiated from the machine [6] and alters the attraction between rotor-stator and changing machines' shaft trajectory [7]. Various diagnostic methods have been developed for the detection of demagnetization based on the frequency signature analysis of machines' [8]–[13] capable not only detecting it but also distinguishing it from eccentricity [14]–[19]. This difficulty appears because the two faults induce on the stator windings harmonic signatures with the same order.

Nevertheless, frequency signature analysis is influenced severely by the winding configuration [20], and the slot number as these harmonics are influenced by the harmonics, which are generated by the slotting effect [18]. Under healthy conditions, the spatial distribution of the coil/pole slot combination significantly affects the harmonic content of voltage through the winding factor [21], in machines with and without armature core. Specifically, in machines with parallel path windings under fault conditions the magnetic field along the air-gap circumference ceases to be symmetric, as a result circulating currents on the branches of a phase generate, distorting the current waveform [22] and influencing the unbalanced magnetic pull [23]. Therefore, the amplitudes of the fault signatures are much dependent on the design parameters of the machine, rendering the diagnostic process unreliable.

Those mentioned above also gave a motive for the development of techniques based on the extraction and process of signals obtained by commercial flux sensors, [24]–[28] or using a number of search coils having proper span along stator's circumference [18], [29]–[33]. Utilizing properly positioned coils has the advantage of exploiting the magnetic flux in specific points on machines' air-gap and taken advantage of the impact of the fault.

Other techniques are based on signal injection at a standstill as a PM motor when it does not produce torque; the q-axis current is zero making it possible to estimate the d-axis current so the d-axis inductance [34]. Inductance varies due to the saturation degree depending on the fault severity and the separation of demagnetization with eccentricity [27]. Furthermore, an online demagnetization state scheme proposed in [35].

Modeling techniques [36], [37] have also been proposed for demagnetization and other faults which make it capable of estimating the demagnetization severity locally on the magnet [38] or for various magnet topologies in both radial-axial flux machines [39].

Under nonstationary speed, the captured signals cease to be periodic, other signal processing algorithms have been proposed for condition monitoring. STFT [40] has a steady window length, so fast transients cannot be analyzed with high resolution and can be combined using Neuro-Fuzzy approach [41]. Therefore, for signals with rapid alterations, Continuous and Discrete Wavelet Transforms (CWT, DWT) are more appropriate as the window length is variable [42][43]. Other time-frequency distributions methods based on the quadratic time-frequency distribution [44], Hilbert-Huang transform, which are capable of analyzing the signal from a time-frequency-energy aspect. Moreover, the demagnetization fault can also be identified using features extracted by CWT and analyzed by the box-counting method and a threshold [45].

There is a significant number of papers that suggest that the location of the demagnetization signatures in the stator current exist at frequencies $f_s \pm k\frac{f_s}{p}$. This paper will prove that this simplified formula can be misleading, because it assumes that all multiples of the mechanical frequency are produced in case of demagnetization. More specifically, this work correlates the cancelation of the harmonic signatures with the coil-winding connection when using the stator current monitoring method based on the signature analysis via the frequency domain. This method is one of the most applicable methods in industrial environments due to its non-intrusiveness, low cost, simplicity and the ability to be applied on-line. This paper is structured as follows. Section II presents the analytical calculation of the voltage in an armature coil due to demagnetization. Section III investigates the cancelation of harmonic signatures analytically due to the spatial distribution of even numbered phase coils. Furthermore, the influence of the three phases connection is also revealed. Section IV follows demonstrating the expected demagnetization signatures in machines with odd numbers of poles and specifically multiple of three. The analytical calculations of all sections are verified and validated in Section V by means of Finite-Element Analysis (FEA) and some experimental testing. Three machines are examined, whereas their geometrical and operating characteristics are very different, thus offering a good level of generalization for this works novel findings. The simulations have been carried out with a commercial software (MagNet). All examined machines are operating as generators under fixed speed, feeding an isolated symmetrical ohmic load. The analysis is transient, while the machines are at steady state and the time step is 0.1 ms. All FEA models of the healthy machines have been verified with experimental results of the real ones. Moreover, one of the machines' simulation results are verified experimentally. Finally, the generalized conclusions are summarized.

II. Magnetic Flux Density due to the Demagnetization

The first step is to establish the magnetic flux density in the air-gap of the PM machine. To calculate that, two components are required: the air-gap permeance and the Magneto-Motive Force (MMF). When those are known then the air-gap flux density is calculated as their product:

$$B_{AG} = \Lambda \cdot \mathcal{F}_m \tag{1}$$

The MMF as a function of space and time is:

$$\mathcal{F}_m(\theta, t) = \sum_{n=2m+1}^{\infty} F_{PM} \cos(np\theta - n\omega_s t - \varphi_n) \tag{2}$$

Furthermore, the permeance function is given as follows if the demagnetization of a single magnet is considered as a pulse rotating with the rotor speed:

$$\Lambda_{dmg}(\theta,t)=\alpha+\beta(D)+\gamma(D)\sum_{k=1}^{\infty}\cos(k\theta-k\omega_r t) \quad (3)$$

where:

$$\alpha=\frac{\mu_o}{2h_{PM}}\left(1-\frac{g}{h_{PM}}-\frac{t_w}{2h_{PM}}+\frac{g^2}{h_{PM}^2}+\frac{gt_w}{h_{PM}^2}+\frac{t_w^2}{4h_{PM}^2}\right)$$

$$\beta(D)=\frac{\mu_o D}{2h_{PM}}\left(\frac{g}{2h_{PM}^2 p}+\frac{t_w}{4h_{PM}p}-\frac{1}{2h_{PM}p}\right)$$

$$\gamma(D)=\frac{\mu_o}{2h_{PM}}\left\{\left(\frac{D}{2h_{PM}p}+\frac{2g}{h_{PM}}+\frac{t_w}{h_{PM}}-1\right)\sum_{k=1}^{\infty}\frac{D}{k\pi h_{PM}}\sin\left(\frac{k\pi}{2p}\right)\right\}$$

The resulting magnetic flux density due to demagnetization is given after substitution of (2) and (3) into (1) as follows:

$$B(\theta,t)=a_k\sum_{n=2m+1}^{\infty}F_{PM}\cos(np\theta-n\omega_s t-\varphi_n)+$$
$$\beta_k\sum_{n=2m+1}^{\infty}\sum_{k=1}^{\infty}F_{PM}A_k\left\{\cos\left[(np-k)\theta-\left(n-\frac{k}{p}\right)\omega_s t-\varphi_n\right]\right.$$
$$\left.+\cos\left[(np+k)\theta-\left(n+\frac{k}{p}\right)\omega_s t-\varphi_n\right]\right\} \quad (4)$$

where:

$$a_k=a+\beta(D)$$

$$\beta_k=\frac{\gamma(D)}{2}$$

Moreover, the magnetic flux is given by:

$$\Phi=\oiint\vec{B}\vec{dS} \quad (5)$$

and due to the change of the magnetic flux, voltage will be induced in the stator coils due to Faraday's Law of Induction:

$$\mathcal{E}=-N\frac{d\Phi}{dt} \quad (6)$$

Considering (4), (5) and (6) together, the induced voltage in the stator coils due to the demagnetization is as follows:

$$V_{dmg}=\sum_{n=2m+1}^{\infty}V_n\cos(np\theta-n\omega_s t-\varphi_n)+$$
$$\sum_{n=2m+1}^{\infty}\sum_{k=1}^{\infty}V_{nk}\left\{\cos\left[(np-k)\theta-\left(n-\frac{k}{p}\right)\omega_s t-\varphi_n\right]+\right.$$
$$\left.\cos\left[(np+k)\theta-\left(n+\frac{k}{p}\right)\omega_s t-\varphi_n\right]\right\} \quad (7)$$

III. Impact of Demagnetization on Machines with Pairs of Coils at 180 Degrees

A. Harmonics Cancellation within a Single Phase

It was shown earlier that the demagnetization will induce voltage harmonics in a single stator coil, according to equation (7). This means that sidebands of frequencies integer multiples of the mechanical frequency are expected around the fundamental voltage harmonic in every coil. In this section, the expected harmonics of a single phase will be revealed, as a function of the number of phase coils and poles number. Moreover, the case of two coils of the same phase is considered. The coils are placed with 180 degrees spatial phase difference to one another. The left sidebands of (7) will be examined first, as described by the term:

$$\sum_{n=2m+1}^{\infty}\sum_{k=1}^{\infty}V_{nk}\cos\left[(np-k)\theta-\left(n-\frac{k}{p}\right)\omega_s t-\varphi_n\right] \quad (8)$$

Furthermore, the number of magnetic pole pairs plays a crucial role on the analysis and will be explained in detail. More specifically, when p is even, the two opposing coils will get the same EMF and so the total voltage due to demagnetization will be:

$$V_{2c\_dmg}=\sum_{n=2m+1}^{\infty}\sum_{k=1}^{\infty}V_{nk}\cos\left[-\left(n-\frac{k}{p}\right)\omega_s t-\varphi_n\right]+$$
$$\sum_{n=2m+1}^{\infty}\sum_{k=1}^{\infty}V_{nk}\cos\left[(np-k)\pi-\left(n-\frac{k}{p}\right)\omega_s t-\varphi_n\right] \quad (9)$$

When p is odd, then the opposing coil pairs should be wound with opposite directions so that the produced EMFs do not cancel out. Therefore, for this case the two voltage components of equation (9) are subtracted and not added.

Now, if p is even the product np is always even because n is always odd. Therefore, 2 cases are examined concerning k. If k is even then the two coil components are in phase, however if it is odd they are opposite and cancel out. On the other hand, if p is odd, then the np is always odd. However, due to the subtraction of the two voltage components, the outcome, which depends on k, is the same as before. The analysis and outcomes are similar for the right hand side sidebands of (7). In summary, when there is a single couple of phase coils at 180 degrees apart, the demagnetization signatures are as follows:

$$f_{dmg}=\left(n\pm\frac{2l}{p}\right)f_s \quad (10)$$

More stator coils will lead to further cancellation of fault signatures. One large family of machines have power of two numbers of phase coils. To examine that, a phase winding consisting of 4 coils is now considered. The coils are located at 90 degrees apart from one another. Based on the previous analysis, the 4 coils will be first grouped in pairs. The first pair includes the coils at 0 and 180 degrees and the other the coils at 90 and 270 degrees. Due to (9) and (10) the two pairs of coils

will get the following voltages induced on the left hand side of the fundamental:

- Pair 1 (0° & 180°)

$$\sum_{n=2m+1}^{\infty}\sum_{l=1}^{\infty} V_{nl}\cos\left[-\left(n-\frac{2l}{p}\right)\omega_s t-\varphi_n\right] \quad (11)$$

- Pair 2 (90° & 270°)

$$\sum_{n=2m+1}^{\infty}\sum_{l=1}^{\infty} V_{nl}\cos\left[(np-2l)\frac{\pi}{2}-\left(n-\frac{2l}{p}\right)\omega_s t-\varphi_n\right] \quad (12)$$

where: $k=2l$ and $V_{nl}=2V_{kl}$.

Considering here, the case of an even pole pair number $p=2b$. Depending on whether b is even or odd, p is expressed as below:

$$p=\begin{cases}4c, & b=even\\ 2(2c+1), & b=odd\end{cases} \quad (13)$$

Furthermore, l can be even $(=2q)$ or odd $(=2q+1)$ as well. At this point there are four different combinations to be considered:

1) if $p=4c$ and $l=2q$
2) if $p=4c$ and $l=2q+1$
3) if $p=2(2c+1)$ and $l=2q$
4) if $p=2(2c+1)$ and $l=2q+1$

Taking into consideration that the two voltage components (11) and (12) need to be added together for even pole pair numbers and subtracted for odd pole pair numbers, it is clear that: Combinations 1 and 3 make the signals (11) and (12) to be in phase, while combinations 2 and 4 lead them to cancel out. To summarize, when there are 4 phase coils at 90 degrees apart, the demagnetization signatures are identified as follows:

$$f_{dmg}=\left(n\pm\frac{4q}{p}\right)f_s \quad (14)$$

Following the same methodology, if 8 coils of a single phase are considered with 45 degrees spatial phase difference, we get:

$$f_{dmg}=\left(n\pm\frac{8r}{p}\right)f_s, \qquad q=2r \quad (15)$$

From the analysis above, it is now clear that the more pairs of coils in the machine, the more the cancelation of the demagnetization signatures. The general rule identified here is the following:

$$\boldsymbol{f_{dmg1}=\left(n\pm\frac{2^{\delta}\cdot\varepsilon}{p}\right)f_s} \quad (16)$$

where δ is equal to the binary logarithm of the number of phase coils and ε is any integer number. It is crucial to mention that, if $2^{\delta}=p$, then the machine does not produce any demagnetization signatures in the stator current around the fundamental, thus the MCSA will lead to a false negative diagnostic outcome.

B. Harmonic Cancellation due to the Three Phase System

So far, it has been shown that, specific locations lead to the cancellation of specific fault signatures. Despite that, PM machines have three phases and the phases themselves have a spatial phase difference of 120 degrees. Moreover, the phases are electrically connected to each other. The logical assumption is therefore that in a 3-phase winding, it is possible that more signatures are cancelled out due to the spatial phase difference between coils of different phases. How this happens is the main question to be answered in this paragraph.

To begin with, a system of 3 coils placed with a spatial phase difference of 120 degrees is examined. Each coil belongs to a different phase and the phases are connected in Y or Δ. Each phase is supplying an equal resistive load. The sum of the three voltages is zero, therefore each phase voltage is equal to the negative sum of the other two. However, it is important to notice that due to the spatial phase difference of 120 degrees, the induced voltages in the two phases have opposite signs. Therefore, the left hand side demagnetization components of the first phase are equal to the difference between the other two phases:

$$V_{3ph\_dmg\_1c}=\sum_{n=2m+1}^{\infty}\sum_{k=1}^{\infty} V_{nk}\left\{\cos\left[(np-k)\frac{2\pi}{3}-\left(n-\frac{k}{p}\right)\omega_s t-\varphi_n\right]-\cos\left[(np-k)\left(-\frac{2\pi}{3}\right)-\left(n-\frac{k}{p}\right)\omega_s t-\varphi_n\right]\right. \quad (17)$$

After changing the signs in the second term and applying trigonometric identities, equation (17) is transformed into:

$$(17)=2\sum_{n=2m+1}^{\infty}\sum_{k=1}^{\infty} V_{nk}\sin\left[(np-k)\frac{2\pi}{3}\right]\times\sin\left[-\left(n-\frac{k}{p}\right)\omega_s t-\varphi_n\right] \quad (18)$$

The first sinusoidal term is zero when:

$$(np-k)\frac{2\pi}{3}=\lambda\pi, \lambda\in\mathbb{Z}\Rightarrow k=np-\frac{3\lambda}{2} \quad (19)$$

At this point it is important to note that, λ can be any integer number. Despite that, $k\in\mathbb{N}$ therefore only even values of λ are of meaning. So, if $\lambda=2\lambda'$:

$$k=np-3\lambda' \quad (20)$$

So, when k obeys to (20), equation (17) is zero and the

respective demagnetization signatures cancel out from the reference phase at 0 degrees. More specifically, after substitution of (20) into (8) we get:

$$\sum_{n=2m+1}^{\infty}\sum_{k=1}^{\infty} V_{nk}\cos\left[-\left(n-\frac{np-3\lambda'}{p}\right)\omega_s t-\varphi_n\right]= \sum_{n=2m+1}^{\infty}\sum_{k=1}^{\infty} V_{nk}\cos\left(\frac{3\lambda'}{p}\omega_s t+\varphi_n\right) \quad (21)$$

Equation (21) demonstrates that signatures that are triple multiples of the mechanical frequency cancel out in the stator current, when all three phases are considered in a PM machine, where each phase consists of a single coil.

Now if each phase consists of more coils, the methodology is similar. More coils simply means an electrical phase difference of 120 degrees between the phases. Therefore, if γ the number of each phase coils, then the demagnetization impact on each phase is:

$$V_{3ph\_dmg}= \sum_{n=2m+1}^{\infty}\sum_{k=1}^{\infty} V_{nk}\left\{\cos\left[(np-k)\frac{2\pi}{3\gamma}-\left(n-\frac{k}{p}\right)\omega_s t-\varphi_n\right]- \cos\left[(np-k)\left(-\frac{2\pi}{3\gamma}\right)-\left(n-\frac{k}{p}\right)\omega_s t-\varphi_n\right]\right. \quad (22)$$

Following a similar methodology to the case of a single coil, equation (22) leads to the conclusion that the number of phase coils leads to the cancellation of demagnetization signatures located at:

$$\boldsymbol{f_{3ph\_null}=\frac{3\gamma\cdot\lambda'}{p}f_s} \quad (23)$$

Equation (23) practically means that, for a machine with 2 coils per phase the sixth multiples of the mechanical frequency will not exist in a 3-phase PM generator suffering from demagnetization. If the phase coils are 4, the twelfth multiples of the mechanical frequency cancel out etc.

IV. Impact of Demagnetization on Machines with Odd Numbers of Coils

As it is not possible to cover every possible topology in detail, this paragraph will focus on the most common case which is that of machines where the coils of every phase are repeated 3 times around the circumference. In such machines, the behavior of the demagnetization will be studied after grouping the coils in teams of 3 coils at 120 degrees.

In this case, the three phase coils will get the same EMF induced, however by a phase difference 120 degrees. As a result, the left hand side demagnetization harmonics of the three connected coils will be:

$$V_{3c\_dmg}= \sum_{n=2m+1}^{\infty}\sum_{k=1}^{\infty} V_{nk}\cos\left[-\left(n-\frac{k}{p}\right)\omega_s t-\varphi_n\right]+ \sum_{n=2m+1}^{\infty}\sum_{k=1}^{\infty} V_{nk}\cos\left[(np-k)\frac{2\pi}{3}-\left(n-\frac{k}{p}\right)\omega_s t-\varphi_n\right]+ \sum_{n=2m+1}^{\infty}\sum_{k=1}^{\infty} V_{nk}\cos\left[(np-k)\left(-\frac{2\pi}{3}\right)-\left(n-\frac{k}{p}\right)\omega_s t-\varphi_n\right] \quad (24)$$

From Eq. (24) it becomes clear that those harmonics will always cancel out when:

$$np-k=\begin{cases}2\zeta\\ 6\zeta\pm 1\end{cases},\zeta\in\mathbb{Z} \quad (25)$$

$$(25)\Rightarrow k=\begin{cases}np-2\zeta\\ np-6\zeta\pm 1\end{cases} \quad (26)$$

Since the components described by (26) disappear, it is evident that each phase produces signatures of the demagnetization fault at frequencies:

$$\boldsymbol{f_{dmg2}=\left(n\pm\frac{3\kappa}{p}\right)f_s},\boldsymbol{\kappa}\in\mathbb{Z} \quad (27)$$

There is of course further cancellation of demagnetization harmonics due to the 3-phase winding. Those are adequately described by the earlier calculated equation (23) which takes into consideration the electrical phase angle difference.

V. Numerical and Experimental Analysis

In order to verify the above analytical investigation, extensive FEA simulations have been carried out with different PM electrical machines. An effort was made to select representative machines to allow for generalization of this paper's conclusions. Therefore, the selected machines are axial and radial, with different numbers of poles and stator windings. The presentation of the results has been organized as follows. Firstly, a multi-pole PM generator will be presented allowing the parametric evaluation of the calculated formulae under different numbers of stator coils. Then results from another 2 and completely different machines in terms of poles and stator coil numbers will be presented. The PM material is the N42 NdFeB and its B-H characteristic for healthy and demagnetized states are shown in Fig. 1.

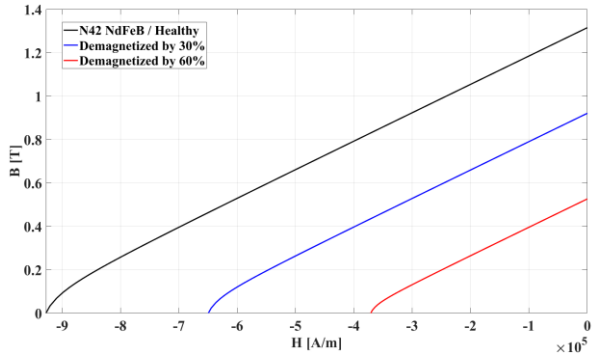

Fig. 1. Te B-H magnetic characteristic of the N42 NdFeB under healthy and demagnetized states.

A. Parametric Analysis of a Radial Flux C-GEN PM Generator (8 stator coils per phase and 16 pole pairs)

The main parametric model which has been used for the analysis represents a C-GEN PM generator for marine energy harvesting. The machine is a radial flux one with two rotors. There are two main reasons behind the selection of this particular machine for this investigation. Firstly, the numerical model of the generator has been experimentally verified in the lab. Secondly, this generator has a significant number of poles (32) due to its inherently very low rotor speed, which is ideal for a parametric investigation on the impact of the coils numbers. The real generator, the magnetic flux distribution under healthy conditions and under partial demagnetization fault under steady state are depicted in Fig. 2. The location of the demagnetized magnet is indicated with a white arrow. Moreover, the characteristics of the generator are shown in Table I. Furthermore, the results from experimental testing and FEA simulation under healthy condition are presented in Table II.

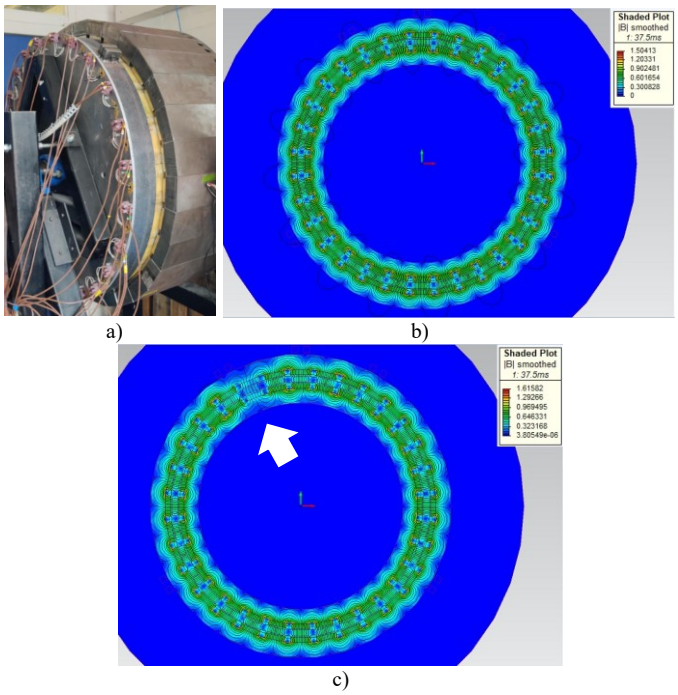

Fig. 2. a) The real C-GEN PM generator in the lab and the magnetic flux density and flux lines distribution under b) healthy and c) demagnetized condition at steady state.

TABLE I
CHARACTERISTICS OF THE C-GEN PM GENERATOR

Rated power	21.5 kW
Rated speed	100 rpm
Stator	Coreless
Frequency	26.67 Hz
Pole pairs	16
Stator coils	24 x single concentrated
Stator coil turns	205
Magnet material	N42 recoil NdFeB

TABLE II
FEA AND TESTING RESULTS

Variable	**FEA**	**Experiment**
Phase voltage (V)	304.3	306.7
Stator current (A)	17.39	17.41
Torque (Nm)	1547	1575
Output Power (kW)	15.9	15.4
Input Power (kW)	16.2	16.5

The generator has been simulated under healthy condition and under partial demagnetization. The demagnetization has been introduced in two opposite magnets and their level is set to 60% for all cases.

Two sets of simulations have been carried out. The first set aims to study the impact of demagnetization on an isolated single phase, while the second set aims for the 3-phase machine. Both sets consider the machine with a single coil, two coils (180°), 4 coils (90°) and 8 coils (45°) per phase.

The simulation results are summarized in the following Fig. 3 and Fig. 4 where the stator current spectra are illustrated for every case while at steady state. When a single phase is considered and consists of a single coil, all multiples of the mechanical frequency exist in the stator current (Fig. 3-a). However, when 3 phases exist and according to equation (21) the triple multiples of the mechanical frequency harmonic do not exist. Moreover, when 2 coils of a single phase exist at 180° (Fig. 3-b), all odd multiples of the mechanical frequency disappear as predicted by equation (16). Additionally, when 3 phases, of two coils each, exist, further cancellation of harmonics located at sixth multiples of the mechanical frequency is observed, obeying to equation (23) because in this case $p' = 2$ (Fig. 4-b).

Increasing the number of phase coils further leads to less demagnetization signatures. According to equation (14), only quadruple multiples of the mechanical frequency are expected for 4 coils per phase, which indeed happens in Fig. 3-c. Similarly, if the coils are 8 (Fig. 3-d), there are only two fault signatures located at $f_s \pm \frac{f_s}{2}$, in accordance to equation (15). However, when all three phases are considered some of those harmonics disappear. Specifically, $p' = 4$ and $p' = 8$ for 4 and 8 coils per phase respectively. Therefore, in the former case, harmonics located at multiples of twelve the mechanical frequency disappear (Fig. 4-c). Moreover, if the phase coils are 8, cancellation of the multiples of 24 the mechanical frequency are expected. This obviously coincides with the right sideband at $f_s + \frac{f_s}{2}$ which cancels out (Fig. 4-d) leaving only the left hand side one to reveal the demagnetization fault. To allow for an easier overview of the fault signatures' locations Tables III and IV are presented below.

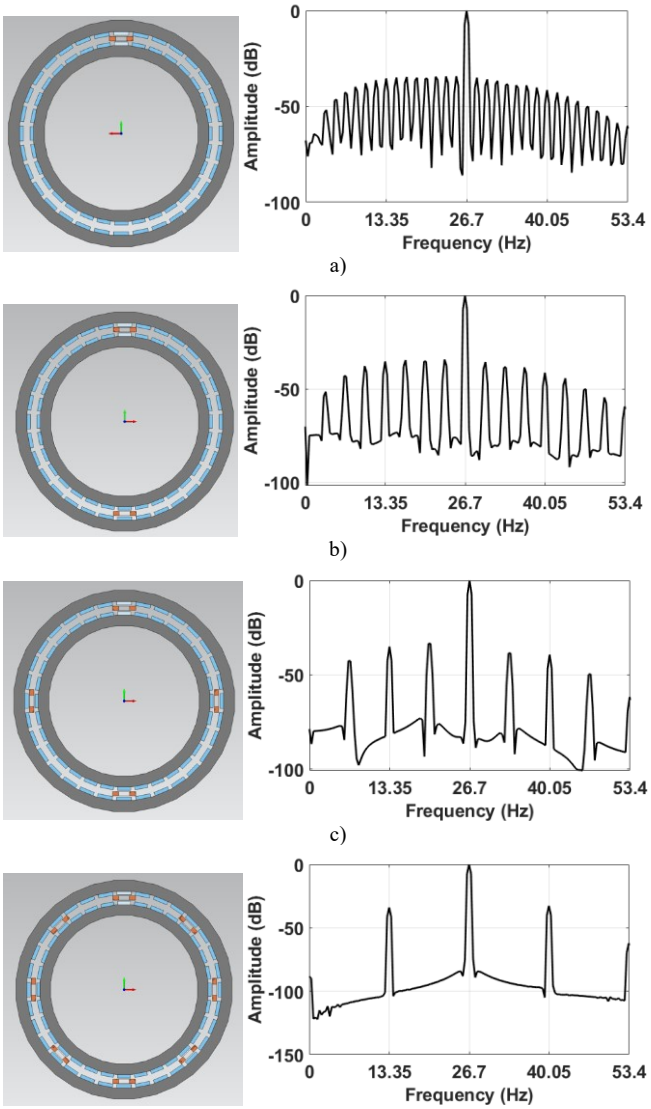

Fig. 3. FFT of the stator current of a PM generator with partial demagnetization at steady state as a function of the number of coils of a single phase: a) 1 coil, b) 2coils, c) 4 coils and d) 8 coils.

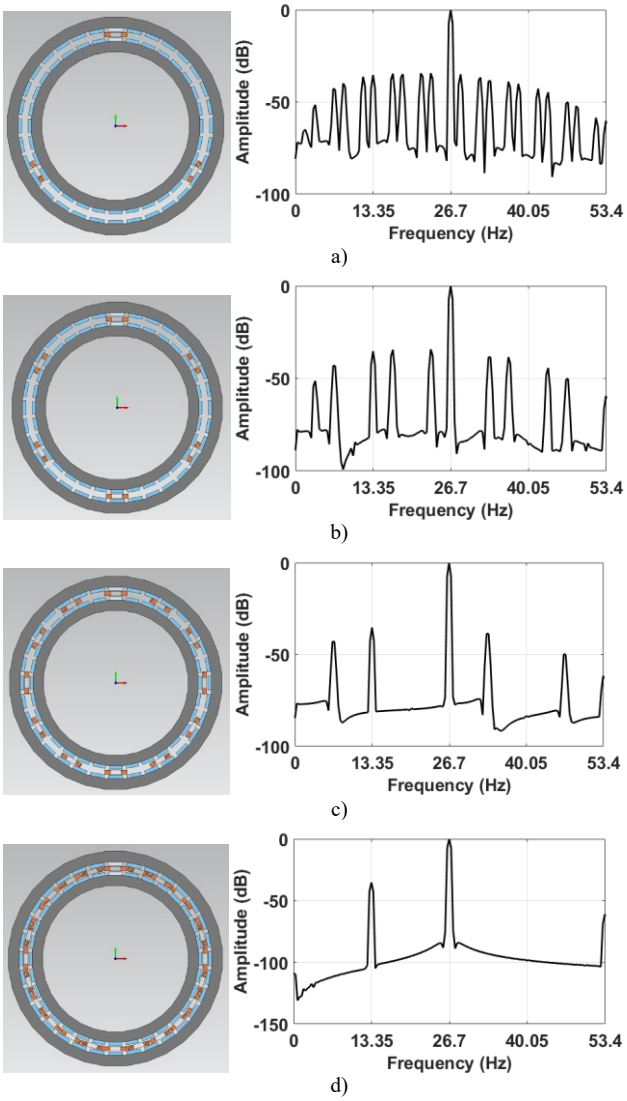

Fig. 4. FFT of the stator current of a PM generator with partial demagnetization at steady state as a function of the number of coils of a machine with 3 phases: a) 1 coil, b) 2coils, c) 4 coils and d) 8 coils.

TABLE III
DEMAGNETIZATION SIGNATURES FOR 1 PHASE (HARMONIC ORDERS OF THE MECHANICAL FREQUENCY AROUND THE FUNDAMENTAL)

1-phase harmonic component																															
Harmonic Order	-16	-15	-14	-13	-12	-11	-10	-9	-8	-7	-6	-5	-4	-3	-2	-1	0	1	2	3	4	5	6	7	8	9	10	11	12	13	14	15	16
1 coil	x	x	x	x	x	x	x	x	x	x	x	x	x	x	x	x	x	x	x	x	x	x	x	x	x	x	x	x	x	x	x	x	x
2 coils	x		x		x		x		x		x		x		x		x		x		x		x		x		x		x		x		x
4 coils	x				x				x				x				x				x				x				x				x
8 coils	x								x								x								x								x

TABLE IV
DEMAGNETIZATION SIGNATURES FOR 3 PHASES (HARMONIC ORDERS OF THE MECHANICAL FREQUENCY AROUND THE FUNDAMENTAL)

3-phase harmonic component																															
Harmonic Order	-16	-15	-14	-13	-12	-11	-10	-9	-8	-7	-6	-5	-4	-3	-2	-1	0	1	2	3	4	5	6	7	8	9	10	11	12	13	14	15	16
1 coil/phase		x	x		x	x		x	x		x	x		x	x		x	x		x	x		x	x		x	x		x	x		x	x
2 coils/phase			x		x				x		x				x		x				x		x				x		x				x
4 coils/phase					x				x								x				x								x				x
8 coils/phase									x								x																x

B. The Case of an Axial Flux PM Generator (3 stator coils per phase and 6 pole pairs)

To further validate the analytical findings, a double rotor, axial flux PM generator with 3 stator coils per phase and 12 magnetic poles has been studied. This particular machine falls under the investigation of paragraph V, as it has odd number of phase coils and specifically 3. The generator has been simulated with FEA and the model is shown in the following Fig. 4. The magnetic flux density distribution under healthy and faulty conditions are also shown. The generator has been simulated under healthy condition and under partial demagnetization fault on one magnet and with fault severity level of 35%.

The stator current spectra have been calculated and presented in Fig. 5 for healthy and faulty operation at steady state. It is clear that the partial demagnetization fault leads to the appearance of strong harmonics at $0.5f_s, 2.5f_s$ and $3.5f_s$ (marked with arrows). Those signatures are the outcome of the combined effect of equations (23) and (27). Since this particular machine has an odd stator coil number as well as a multiple of 3, all demagnetization harmonics but the triple multiples of the mechanical frequency will disappear. Therefore, on the fundamental's left hand side, only the 3rd multiple of the mechanical frequency is expected to appear. Since the number of pole pairs is 6, this leads to the signature at $0.5f_s$. Despite that, the right hand signature at $1.5f_s$ is cancelled due to the three phase stator connection, obeying to equation (23) for $\gamma = 3$. The signatures at $2.5f_s$ and $3.5f_s$ originate from equation (27) as well because they are both triple multiples of the mechanical frequency. Moreover, they are not multiples of 9 and therefore they are excluded from cancellation due to equation (23).

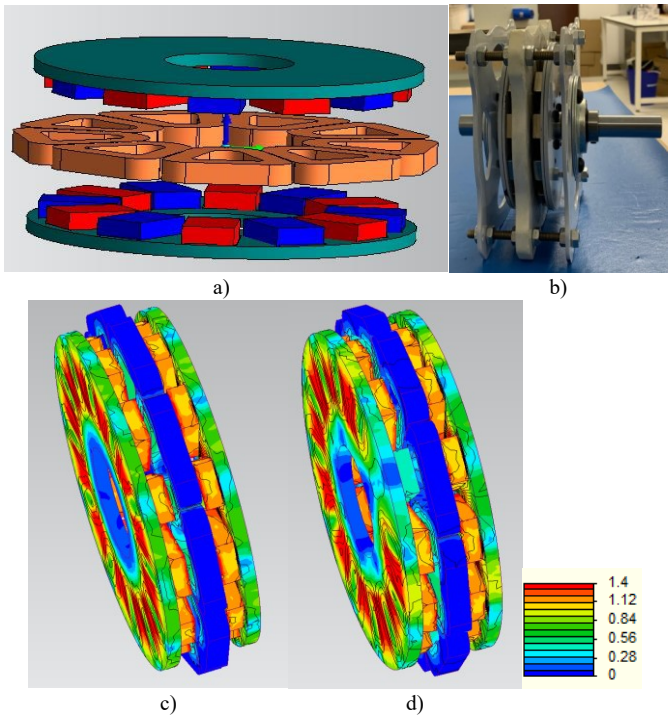

Fig. 4. a) The FEA model of the axial flux PM generator with 3 coils per phase and 6 pole pairs, b) the real machine and the magnetic flux distribution under: c) healthy and d) faulty condition.

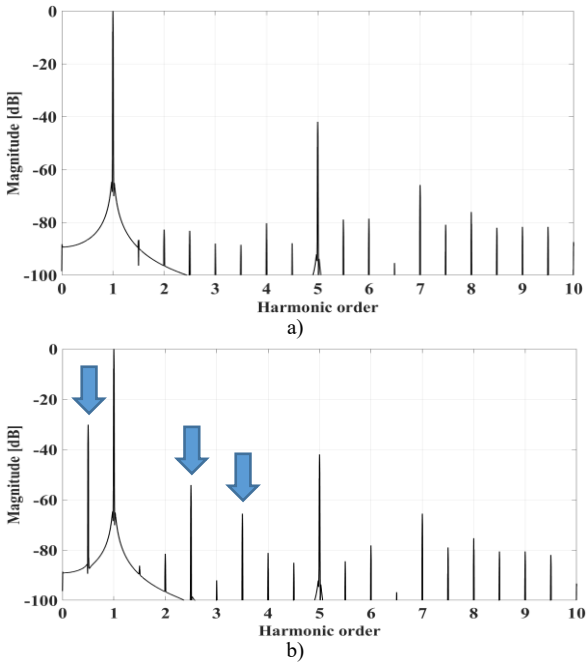

Fig. 5. Stator current spectra of an axial flux PM generator with 3 coils per phase and 6 pole pairs: a) healthy and b) faulty with partial demagnetization.

This machine has been tested experimentally under healthy conditions and under 50% demagnetization fault. The test rig is shown in Fig. 6. The PM generator is rotated by an induction motor fed by an inverter. The generator feeds into a symmetrical 3-phase ohmic load. The stator currents are recorded with a portable picoscope and installed current sensors.

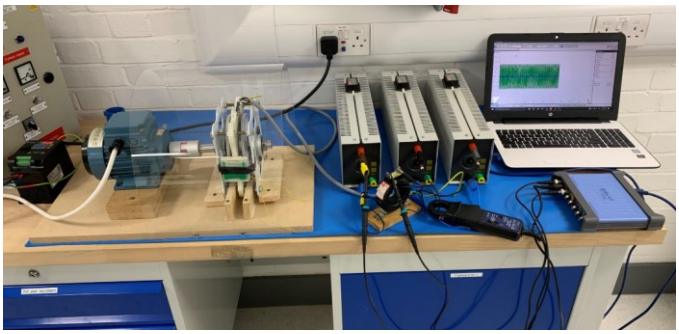

Fig. 6. The test rig to measure the healthy and faulty AFPM generator with 3 coils per phase and 6 pole pairs.

The spectra of the stator currents at steady state are shown in the following Fig. 7. The three signatures, predicted by FEA earlier, at $0.5f_s, 2.5f_s$ and $3.5f_s$ increase in amplitude in the faulty machine (marked with arrows). More specifically, the $0.5f_s$ component's amplitude is -29.2 dB, the $2.5f_s$ one is at -40.9 dB and the $3.5f_s$ is at -53.6 dB. The amplitude increase compared to the healthy state is approximately 15 dB for all three signatures. The experimental results verify the analytical calculations and simulation results satisfactorily.

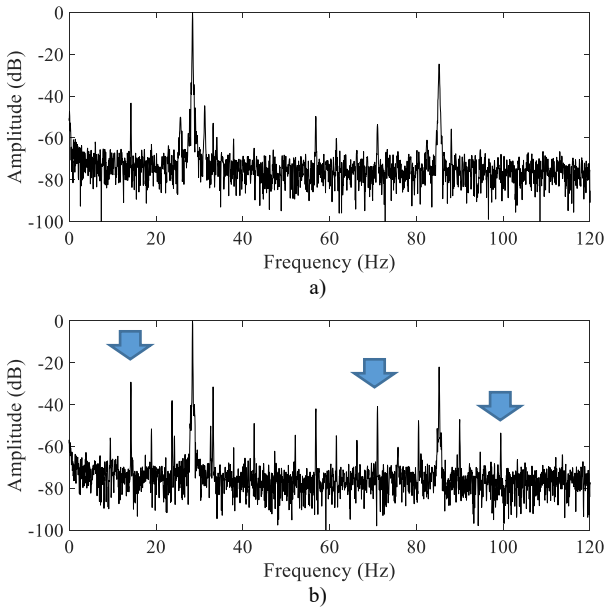

Fig. 7. Frequency spectra of the stator current at steady state extracted from the AFPM generator with 3 coils per phase and 6 pole pairs under: a) healthy state and b) 50% partial demagnetization fault.

C. The Case of an Axial Flux C-GEN PM Generator (12 stator coils per phase and 24 pole pairs)

The final case of this paper is that of an axial flux PM generator with 12 coils per phase and 48 poles (Fig. 8). It is an interesting case because it combines the characteristics of the previous two studied cases. That is because it has coils at 180 degrees apart and at the same time the number of coils is a multiple of 3. Therefore, the combined effect of equations (16), (23) and (27) is expected to act in the generation or cancellation of the demagnetization harmonics of the stator current.

a) b)

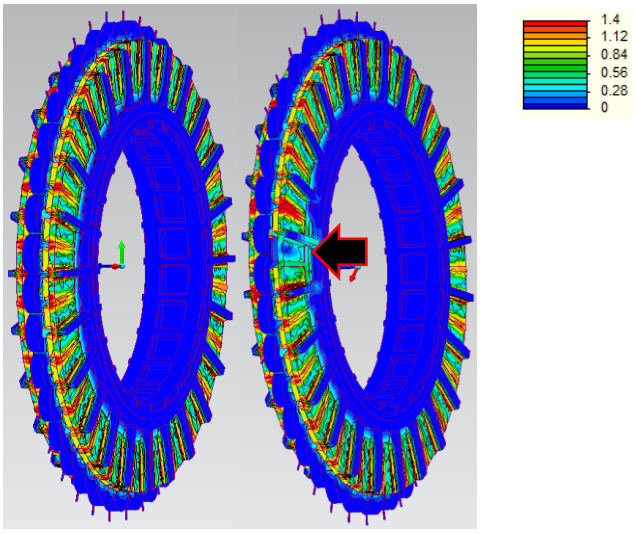

c) d)

Fig. 8. a) The FEA model of the axial flux PM generator with 12 coils per phase and 24 pole pairs, b) the real machine and the magnetic flux distribution under: c) healthy and d) faulty condition.

Since, $p = 24$, each coil on its own will produce all multiples of the mechanical frequency $\nu \cdot \left({}^{f_s}/_{p}\right), \nu \in \mathbb{Z}$ as sidebands to the fundamental stator current harmonic. However, each phase consists of 12 coils. 12 is a multiple of 4 and 3. Therefore, according to equation (16), the first couple of coils at 180 degrees will cancel out the odd multiples of the mechanical frequency while the second couple at 90 and 270 degrees will cancel all even multiples of 2 and an odd number. This harmonic cancellation leaves only signatures multiples of 4 and therefore $\nu \in (4,8,12,16,20)$ on the left of the fundamental.

However, the number of phase coils is also a multiple of 3. Therefore, according to equation (23), all demagnetization signatures, but the multiples of three, cancel out from the spectrum. From the 5 possible values of ν, only one is a multiple of 3. All others cancel out. So, the only signature that this machine is expected to have on the left of the fundamental of the stator current is the $f_s - \frac{12 f_s}{24} = 0.5 f_s$.

The approach is similar for the signatures to the right of the fundamental. There is only one fault signature between f_s and $2f_s$ considering the simultaneous effect of equations (16) and (23) and this is the $f_s + \frac{36 f_s}{24}$, since 36 is multiple of both 3 and 4. However, the application of equation (27) forces the cancelation of multiples of 36 from the current spectrum. Therefore, no mechanical frequency related signatures are expected on the right hand side of the fundamental. A closer look though reveals that the second harmonic of the current is the 48th multiple of the mechanical frequency and 48 is multiple of 3 and 4 while not a multiple of 36. So, the amplitude of the $2f_s$ harmonic is expected to increase due to the demagnetization fault. This is an interesting result since the increase of the second current harmonic has been associated with stator faults and imbalances of the three phase winding such as inter-turn faults, supply imbalance, high resistance connections etc. This is the first time that this signature is directly associated with faults originating from the rotor.

The results from the numerical analysis are most satisfying as shown below (Fig. 9). As predicted by the analytical formulae, the $0.5f_s$ and $2f_s$ harmonics increase when there is partial demagnetization in the machine with 12 coils/phase and 48 poles.

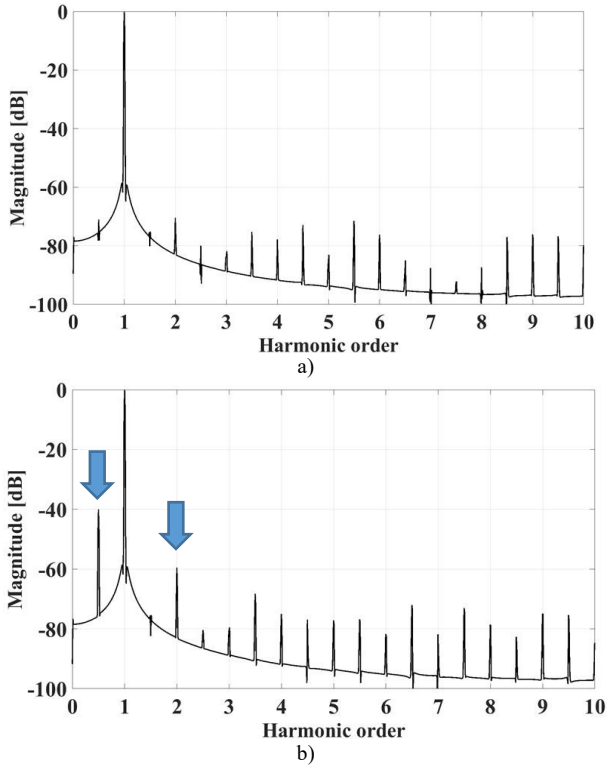

Fig. 9. Stator current spectra of an axial flux PM generator with 12 coils per phase and 24 pole pairs: a) healthy and b) faulty with partial demagnetization.

VI. Conclusion

The paper presents an analytical investigation of the partial demagnetization harmonics expected in the stator current of PM machines as a function of the numbers of poles and coils per phase. It has been proved that the expected harmonics mainly depend on the number of phase coils, which when increases leads to less signatures in the stator current spectra. The useful flux direction does not play any role and the analytical investigation is valid for both radial and axial flux PM machines. Furthermore, the 3-phase connection between the phases leads to additional cancellation of fault signatures. The analytical investigation has been fully verified with extensive FEA simulations for the case of three different PM generators selected to generalize the proposed methodology. Considering that multiple rotor faults of PM machines are expressed as functions of the mechanical frequency (eccentricity, misalignment, bearing faults etc.), identification of the harmonics' origin is of the outmost importance to plan remedy actions accordingly and before a catastrophic machine breakdown. Moreover, the paper's findings suggest that the second stator current harmonic may be demagnetization related, a finding that poses a new challenge; that of discriminating stator faults from rotor demagnetizations ones. To conclude, this paper's original contribution aims towards the reliable identification of the demagnetization as a function of the machine's manufacturing parameters and characteristics. Future work will focus on the identification of the partial demagnetization in PM machines with distributed windings.

Appendix

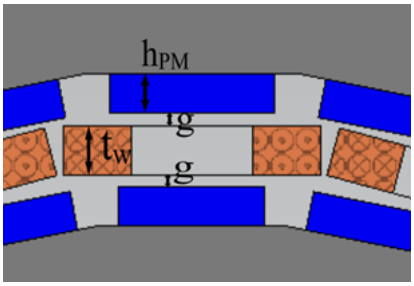

The parameters h_{PM}, t_w and g in the radial flux machine required for the calculation of $\alpha, \beta(D)$ and $\gamma(D)$.

References

[1] J. Faiz and E. Mazaheri-Tehrani, "Demagnetization Modeling and Fault Diagnosing Techniques in Permanent Magnet Machines under Stationary and Nonstationary Conditions: An Overview," *IEEE Trans. Ind. Appl.*, vol. 53, no. 3, pp. 2772–2785, 2017.

[2] J. Faiz and H. Nejadi-Koti, "Demagnetization Fault Indexes in Permanent Magnet Synchronous Motors-An Overview," *IEEE Trans. Magn.*, vol. 52, no. 4, 2016.

[3] J. Hong, D. Hyun, S. Bin Lee, J. Y. Yoo, and K. W. Lee, "Automated monitoring of magnet quality for permanent-magnet synchronous motors at standstill," *IEEE Trans. Ind. Appl.*, vol. 46, no. 4, pp. 1397–1405, 2010.

[4] S. Ruoho, J. Kolehmainen, J. Ikäheimo, and A. Arkkio, "Interdependence of demagnetization, loading, and temperature rise in a permanent-magnet synchronous motor," *IEEE Trans. Magn.*, vol. 46, no. 3 PART 2, pp. 949–953, 2010.

[5] J. D. McFarland and T. M. Jahns, "Investigation of the rotor demagnetization characteristics of interior PM synchronous machines during fault conditions," *IEEE Trans. Ind. Appl.*, vol. 50, no. 4, pp. 2768–2775, 2014.

[6] D. Torregrossa, A. Khoobroo, and B. Fahimi, "Prediction of acoustic noise and torque pulsation in PM synchronous machines with static eccentricity and partial demagnetization using field reconstruction method," *IEEE Trans. Ind. Electron.*, vol. 59, no. 2, pp. 934–944, 2012.

[7] J. C. Urresty, R. Atashkhooei, J. R. Riba, L. Romeral, and S. Royo, "Shaft trajectory analysis in a partially demagnetized permanent-magnet synchronous motor," *IEEE Trans. Ind. Electron.*, vol. 60, no. 8, pp. 3454–3461, 2013.

[8] J. C. Urresty, J. R. Riba, and L. Romeral, "A back-emf based method to detect magnet failures in PMSMs," *IEEE Trans. Magn.*, vol. 49, no. 1, pp. 591–598, 2013.

[9] J. C. Urresty, J. R. Riba, M. Delgado, and L. Romeral, "Detection of demagnetization faults in surface-mounted permanent magnet synchronous motors by means of the zero-sequence voltage component," *IEEE Trans. Energy Convers.*, vol. 27, no. 1, pp. 42–51, 2012.

[10] J. De Bisschop, A. A. E. Abdallh, P. Sergeant, and L. Dupré, "Analysis and selection of harmonics sensitive to demagnetisation faults intended for condition monitoring of double rotor axial flux permanent magnet synchronous machines," *IET Electr. Power Appl.*, vol. 12, no. 4, pp. 486–493, 2018.

[11] W. Le Roux, R. G. Harley, and T. G. Habetler, "Detecting rotor faults in permanent magnet synchronous machines," *IEEE Int. Symp. Diagnostics Electr. Mach. Power Electron. Drives, SDEMPED 2003 - Proc.*, vol. 22, no. 1, pp. 198–203, 2003.

[12] J. Bossio, C. Ruschetti, G. Bossio, C. Verucchi, and C. De Angelo, "Rotor fault diagnosis in permanent magnet synchronous machine using the midpoint voltage of windings," *IET Electr. Power Appl.*, vol. 14, no. 2, pp. 256–261, 2020.

[13] B. M. Ebrahimi and J. Faiz, "Demagnetization fault diagnosis in surface mounted permanent magnet synchronous motors," *IEEE Trans. Magn.*, vol. 49, no. 3, pp. 1185–1192, 2013.

[14] S. Rajagopalan, W. le Roux, T. G. Habetler, and R. G. Harley, "Dynamic eccentricity and demagnetized rotor magnet detection in trapezoidal flux (Brushless DC) motors operating under different load conditions," *IEEE Trans. Power Electron.*, vol. 22, no. 5, pp. 2061–2069, 2007.

[15] Z. Liu, J. Huang, and B. Li, "Diagnosing and distinguishing rotor eccentricity from partial demagnetisation of interior PMSM based on fluctuation of high-frequency d-axis inductance and rotor flux," *IET Electr. Power Appl.*, vol. 11, no. 7, pp. 1265–1275, 2017.

[16] R. Z. Haddad and E. G. Strangas, "On the Accuracy of Fault Detection and Separation in Permanent Magnet Synchronous Machines Using MCSA/MVSA and LDA," *IEEE Trans. Energy Convers.*, vol. 31, no. 3, pp. 924–934, 2016.

[17] T. Goktas, M. Zafarani, and B. Akin, "Discernment of Broken Magnet and Static Eccentricity Faults in Permanent Magnet Synchronous Motors," *IEEE Trans. Energy Convers.*, vol. 31, no. 2, pp. 578–587, 2016.

[18] T. Goktas, M. Zafarani, K. W. Lee, B. Akin, and T. Sculley, "Comprehensive Analysis of Magnet Defect Fault Monitoring Through Leakage Flux," *IEEE Trans. Magn*., vol. 53, no. 4, 2017.

[19] M. Zafarani, T. Goktas, and B. Akin, "A comprehensive magnet defect fault analysis of permanent magnet synchronous motors," *IEEE Trans. Ind. Appl.*, vol. 2015, no. 2, pp. 1331–1339, 2015.

[20] J. C. Urresty, J. R. Riba, and L. Romeral, "Influence of the stator windings configuration in the currents and zero-sequence voltage harmonics in permanent magnet synchronous motors with demagnetization faults," *IEEE Trans. Magn.*, vol. 49, no. 8, pp. 4885–4893, 2013.

[21] M. J. Kamper, A. J. Rix, D. A. Wills, and R. J. Wang, "Formulation, finite-element modeling and winding factors of non-overlap winding permanent magnet machines," *Proc. 2008 Int. Conf. Electr. Mach. ICEM'08*, no. 3, pp. 1–5, 2008.

[22] E. Maruyama, A. Nakahara, A. Takahashi, and K. Miyata, "Circulating current in parallel connected stator windings due to rotor eccentricity in permanent magnet motors," *2013 IEEE Energy Convers. Congr. Expo. ECCE 2013*, pp. 2850–2855, 2013.

[23] I. P. Brown, D. M. Ionel, and D. G. Dorrell, "Influence of parallel paths on current-regulated sine-wave interior-permanent-magnet machines with rotor eccentricity," *IEEE Trans. Ind. Appl.*, vol. 48, no. 2, pp. 642–652, 2012.

[24] Y. Park *et al.*, "Online detection and classification of rotor and load defects in PMSMs Based on Hall sensor measurements," *IEEE Trans. Ind. Appl.*, vol. 55, no. 4, pp. 3803–3812, 2019.

[25] D. Reigosa, D. Fernandez, Y. Park, A. B. Diez, S. Bin Lee, and F. Briz, "Detection of Demagnetization in Permanent Magnet Synchronous Machines Using Hall-Effect Sensors," *IEEE Trans. Ind. Appl.*, vol. 54, no. 4, pp. 3338–3349, 2018.

[26] D. Reigosa, D. Fernandez, M. Martinez, Y. Park, S. Bin Lee, and F. Briz, "Permanent Magnet Synchronous Machine Non-Uniform Demagnetization Detection Using Zero-Sequence Magnetic Field Density," *IEEE Trans. Ind. Appl.*, vol. 55, no. 4, pp. 3823–3833, 2019.

[27] J. Hong *et al.*, "Detection and classification of rotor demagnetization and eccentricity faults for PM synchronous motors," *IEEE Trans. Ind. Appl.*, vol. 48, no. 3, pp. 923–932, 2012.

[28] A. Mohammed, J. I. Melecio, and S. Durovic, "Electrical Machine Permanent Magnets Health Monitoring and Diagnosis Using an Air-Gap Magnetic Sensor," *IEEE Sens. J.*, vol. 20, no. 10, pp. 5251–5259, 2020.

[29] S. M. Mirimani, A. Vahedi, F. Marignetti, and R. Di Stefano, "An online method for static eccentricity fault detection in axial flux machines," *IEEE Trans. Ind. Electron.*, vol. 62, no. 3, pp. 1931–1942, 2015.

[30] Y. Da, X. Shi, and M. Krishnamurthy, "A new approach to fault diagnostics for permanent magnet synchronous machines using electromagnetic signature analysis," *IEEE Trans. Power Electron.*, vol. 28, no. 8, pp. 4104–4112, 2013.

[31] K. Kang, J. Song, C. Kang, S. Sung, and G. Jang, "Real-Time Detection of the Dynamic Eccentricity in Permanent-Magnet Synchronous Motors by Monitoring Speed and Back EMF Induced in an Additional Winding," *IEEE Trans. Ind. Electron.*, vol. 64, no. 9, pp. 7191–7200, 2017.

[32] M. Irhoumah, R. Pusca, E. Lefevre, D. Mercier, and R. Romary, "Detection of the Stator Winding Inter-Turn Faults in Asynchronous and Synchronous Machines Through the Correlation between Harmonics of the Voltage of Two Magnetic Flux Sensors," *IEEE Trans. Ind. Appl.*, vol. 55, no. 3, pp. 2682–2689, 2019.

[33] J. Penman, H. G. Sedding, B. A. Lloyd and W. T. Fink, "Detection and location of interturn short circuits in the stator windings of operating motors," *IEEE Trans. Energy Convers.*, vol. 9, no. 4, pp. 652–658, 1994.

[34] J. Hong, S. Bin Lee, C. Kral, and A. Haumer, "Detection of airgap eccentricity for permanent magnet synchronous motors based on the d-axis inductance," *IEEE Trans. Power Electron.*, vol. 27, no. 5, pp. 2605–2612, 2012.

[35] D. Díaz Reigosa, D. Fernandez, Z. Q. Zhu, and F. Briz, "PMSM Magnetization State Estimation Based on Stator-Reflected PM Resistance Using High-Frequency Signal Injection," *IEEE Trans. Ind. Appl.*, vol. 51, no. 5, pp. 3800–3810, 2015.

[36] E. Ajily, M. Ardebili, and K. Abbaszadeh, "Magnet Defect and Rotor Eccentricity Modeling in Axial-Flux Permanent-Magnet Machines via 3-D Field Reconstruction Method," *IEEE Trans. Energy Convers.*, vol. 31, no. 2, pp. 486–495, 2016.

[37] M. Dai, A. Keyhani, and T. Sebastian, "Fault analysis of a PM brushless DC motor using finite element method," *IEEE Trans. Energy Convers.*, vol. 20, no. 1, pp. 1–6, 2005.

[38] J. A. Farooq, A. Djerdir, and A. Miraoui, "Analytical modeling approach to detect magnet defects in permanent-magnet brushless motors," *IEEE Trans. Magn.*, vol. 44, no. 12, pp. 4599–4604, 2008.

[39] B. Guo, Y. Huang, F. Peng, and J. Dong, "General Analytical Modeling for Magnet Demagnetization in Surface Mounted Permanent Magnet Machines," *IEEE Trans. Ind. Electron.*, vol. 66, no. 8, pp. 5830–5838, 2019.

[40] E. G. Strangas, S. Aviyente, and S. S. H. Zaidi, "Time-frequency analysis for efficient fault diagnosis and failure prognosis for interior permanent-magnet AC motors," *IEEE Trans. Ind. Electron.*, vol. 55, no. 12, pp. 4191–4199, 2008.

[41] M. A. Awadallah, M. M. Morcos, S. Gopalakrishnan, and T. W. Nehl, "A neuro-fuzzy approach to automatic diagnosis and location of stator inter-turn faults in CSI-fed PM brushless DC motors," *IEEE Trans. Energy Convers.*, vol. 20, no. 2, pp. 253–259, 2005.

[42] J. R. Riba Ruiz, J. A. Rosero, A. Garcia Espinosa, and L. Romeral, "Detection of demagnetization faults in permanent-Magnet synchronous motors under nonstationary conditions," *IEEE Trans. Magn.*, vol. 45, no. 7, pp. 2961–2969, 2009.

[43] M. A. Awadallah, M. M. Morcos, S. Gopalakrishnan, and T. W. Nehl, "Detection of stator short circuits in VSI-Fed brushless DC motors using wavelet transform," *IEEE Trans. Energy Convers.*, vol. 21, no. 1, pp. 1–8, 2006.

[44] S. Rajagopalan, J. A. Restrepo, J. M. Aller, T. G. Habetler, and R. G. Harley, "Nonstationary motor fault detection using recent quadratic time-frequency representations," *IEEE Trans. Ind. Appl.*, vol. 44, no. 3, pp. 735–744, 2008.

[45] M. Delgado Prieto, A. Garcia Espinosa, J. R. Riba Ruiz, J. C. Urresty, and J. A. Ortega, "Feature Extraction of demagnetization faults in permanent-magnet synchronous motors based on box-counting fractal dimension," *IEEE Trans. Ind. Electron.*, vol. 58, no. 5, pp. 1594–1605, 2011.

BIOGRAPHIES

Konstantinos N. Gyftakis (M'11, SM'20) received the Diploma in Electrical and Computer Engineering from the University of Patras, Patras, Greece in 2010. He pursued a Ph.D in the same institution in the area of electrical machines condition monitoring and fault diagnosis (2010-2014). Furthermore, he worked as a Post-Doctoral Research Assistant in the Dept. of Engineering Science, University of Oxford, UK (2014-2015). Then he worked as Lecturer (2015-2018) and Senior Lecturer (2018-2019) in the School of Computing, Electronics and Mathematics and as an Associate with the Research Institute for Future Transport and Cities, Coventry University, UK.

Since 2019, he has been a Lecturer in Electrical Machines and a Member of the Institute for Energy Systems, University of Edinburgh, UK.

His research interests focus in the fault diagnosis, condition monitoring and degradation of electrical machines. He has authored/co-authored more than 100 papers in international scientific journals and conferences and a chapter for the

book: “Diagnosis and Fault Tolerance of Electrical Machines, Power Electronics and Drives”, IET, 2018. He is an IEEE Senior Member, as well as member of the IEEE IAS and IEEE IES.

Syidy Rasid was born in Butterworth, Penang, Malaysia, in 1979. He received the BTEC Higher National Diploma in instrumentation and control from the University of Wales College Newport, UK, in 2000; B.Eng degree in electrical and electronic engineering from the University of Derby, UK, in 2014. He is currently working toward a Ph.D. degree at the University of Edinburgh, UK.

He founded Infinity Contracting, Shah Alam, Malaysia involving in power plant maintenance and consultancy for Tenaga Nasional Berhad (TNB), Malaysia.

His research interests include condition monitoring, electrical machines and electric vehicle traction and propulsion. He is an IEEE Student Member, the IET Member as well as member of the IEEE IAS and IEEE IES.

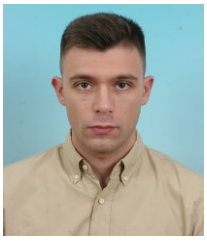

Giorgos A. Skarmoutsos (S’20) was born in Athens, Greece in August 1995. He received the diploma degree in electrical and computer engineering from University of Patras, Greece in 2018. He is currently working toward the Ph.D. degree in electrical engineering at the Institute for Energy Systems, The University of Edinburgh, Edinburgh, U.K. His research is oriented on the analytical modeling, field computation and diagnostic techniques of axial flux machines.

Markus Mueller received the B.Sc. (Eng.) degree from Imperial College London, London, U.K., and the Ph.D. degree from the University of Cambridge, Cambridge, U.K., in 1988 and 1991, respectively. He was a Lecturer with the School of Engineering, University of Durham, from 1997 to 2004. Since 2004, he has been with the School of Engineering, University of Edinburgh, where he holds a Personal Chair in electrical generation systems and was the Head of the Institute for Energy Systems, 2014–2018.